The Astrophysical Journal, 961:17 (5pp), 2024 January 20 https://doi.org/10.3847/1538-4357/ad1035

Constraints on Coasting Cosmological Models from Gravitational-wave Standard Sirens

Peter Raffai[1,2], Mária Pálfi[1], Gergely Dályа[3], and Rachel Gray[4]
[1] Institute of Physics and Astronomy, ELTE Eötvös Loránd University, 1117 Budapest, Hungary; peter.raffai@ttk.elte.hu
[2] HUN-REN-ELTE Extragalactic Astrophysics Research Group, 1117 Budapest, Hungary
[3] Department of Physics and Astronomy, Universiteit Gent, B-9000 Ghent, Belgium
[4] SUPA, University of Glasgow, Glasgow, G12 8QQ, UK
Received 2023 October 25; accepted 2023 November 25; published 2024 January 11

Abstract

We present the first test of coasting cosmological models with gravitational-wave (GW) standard sirens observed in the first three observing runs of the LIGO–Virgo–KAGRA detector network. We apply the statistical galaxy catalog method adapted to coasting cosmologies and infer constraints on the H_0 Hubble constant for the three fixed values of the curvature parameter $k = \{-1, 0, +1\}$ in $H_0^2 c^{-2}$ units. The maximum posteriors and 68.3% highest density intervals we obtained from a combined analysis of 46 dark siren detections and a single bright siren detection are $H_0 = \{68.1^{+8.5}_{-5.6}, 67.5^{+8.3}_{-5.2}, 67.1^{+6.6}_{-5.8}\}$ km s^{-1} Mpc^{-1}, respectively. All our constraints on H_0 are consistent within 1σ with the H_0 measured with the differential age method, which provides a constraint on H_0 in coasting cosmologies independently from k. Our results constrain all cosmological models with $a(t) \propto t$ linear expansion in the luminosity distance and redshift range of the 47 LIGO–Virgo detections, i.e., $d_L \lesssim 5$Gpc and $z \lesssim 0.8$, which practically include all (both strictly linear and quasi-linear) models in the coasting model family. As we have found, the coasting models and the Lambda cold dark matter (or ΛCDM) model fit equally well to the applied set of GW detections.

Unified Astronomy Thesaurus concepts: Gravitational wave astronomy (675); Cosmology (343); Observational cosmology (1146); Hubble constant (758)

1. Introduction

Coasting cosmologies is a family of cosmological models with the common feature that the $a(t)$ scale factor grows linearly with cosmic time t (see Casado 2020 for a review). Such models include ones suggesting strictly $a(t) \propto t$ linear expansion for the universe from the Big Bang to the present cosmic time, while in quasi-linear models the universe follows an evolution similar to the one in the current concordance model of cosmology (termed the Lambda cold dark matter, or ΛCDM, model; see Peebles & Ratra 2003 for a review) at early times and smoothly transitions to linear expansion around a late time and redshift $z_c < z_*$, where z_* is the redshift at recombination (Aghanim et al. 2020). Members of the coasting model family differ in the physical principles or mechanisms they propose as being responsible for the linear expansion, and/or in the value of the k spatial curvature they suggest or allow. For example, the dynamics proposed by the earliest coasting model, developed by Arthur Milne in the 1930s (Milne 1935), resembles that of an empty ($\rho = 0$) universe with zero Λ cosmological constant and negative k. A more recent example for a universe with linear expansion and $k = -1$ is given by the Dirac–Milne model (Benoit-Lévy & Chardin 2012). Other coasting models, such as the $R_h = ct$ model (Melia 2007; Melia & Shevchuk 2012; Melia 2020a) and the eternal coasting model by John and Joseph (John & Joseph 1996, 2000) suggest $k = 0$ and $k = +1$, respectively, although their core postulates allow any other value for k (see, e.g., John & Joseph 2000, 2023).

There are both theoretical and empirical motivations for studying coasting models even in view of the yet unparalleled success of the ΛCDM model. Coasting models provide natural solutions to several known theoretical problems in the ΛCDM model, including the horizon, the flatness, the cosmological constant, the synchronicity, the cosmic coincidence, and the cosmic age problems (see Casado 2020 for a review). Note, however, that the horizon and flatness problems are solved by the ΛCDM model when extended with the theory of cosmic inflation (Guth 1981; Baumann 2009), while others in the list may simply be unlikely coincidences in the realizations of ΛCDM model parameters rather being problems in the model itself. Yet, the recently confirmed tensions between the H_0 Hubble constant (Riess 2020) and the S_8 structure growth parameter (Di Valentino et al. 2021) measured locally and determined from cosmic microwave background (CMB) observations using the ΛCDM model (Aghanim et al. 2020), as well as other anomalies (Perivolaropoulos & Skara 2022), may also signify the need for studying alternatives to the current concordance model of cosmology. Coasting models fit remarkably well to a wide range of cosmological data sets at low ($z \ll z_*$) redshifts (see, e.g., in Table 2 of Melia 2018 and references therein). Strictly linear models, however, have difficulties in explaining the observed abundances of light chemical elements presumably set by the process of primordial nucleosynthesis in the early Universe (Kaplinghat et al. 1999; Sethi et al. 1999; Kaplinghat et al. 2000; Lewis et al. 2016), as well as the origin and properties of anisotropies observed in the CMB (see, e.g., Melia 2020b; Fujii 2020; Melia 2022), both of which are well elaborated and understood in the framework of the ΛCDM model (Dodelson 2003). Another limitation of coasting models is that the new physics they propose is testable only on cosmological scales, and thus far they lack predictions that are within the reach of laboratory-scale experiments.

Since achieving the first detection of gravitational waves (GWs) in 2015 (Abbott et al. 2016), the Advanced LIGO (Aasi et al. 2015), Advanced Virgo (Acernese et al. 2015), and KAGRA (Akutsu et al. 2021) detectors have completed three observing runs, detecting a total of 90 GW signals from coalescing compact binaries (Abbott et al. 2021b). The detections included GW170817 (Abbott et al. 2017a), a GW signal from a binary neutron star merger for which electromagnetic counterparts in various bands have also been found (Abbott et al. 2017b). The exact localization of the optical counterpart allowed the identification of the host galaxy of this event (Abbott et al. 2017b), and the precise determination of its cosmological redshift (Abbott et al. 2017c), earning the term *bright siren* for the GW source. So far, GW170817 has remained the only GW signal with an associated host, with all others originating from *dark sirens*, i.e., coalescing compact binaries with detected GW emissions but no electromagnetic counterparts. As Schutz (1986) pointed out, the d_L luminosity distances of coalescing compact binaries can be inferred from their GW signals without the need for a distance calibrator, which makes them what we call *standard sirens* (Holz & Hughes 2005). Standard sirens with identified host galaxies or with a set of possible host galaxies can be used to test the $d_L(z)$ redshift versus distance relationship of a selected cosmological model, as well as to constrain the model parameters, most prominently the rate of expansion at present time, i.e., the H_0 Hubble constant (Dalal et al. 2006; MacLeod & Hogan 2008; Nissanke et al. 2013). Such constraints on parameters of the ΛCDM model have already been published by the LIGO–Virgo–KAGRA Collaboration (Abbott et al. 2017c; Soares-Santos et al. 2019; Abbott et al. 2021a, 2023a).

In this paper, we present the first attempt to use GW standard sirens for testing coasting cosmologies, and to infer H_0 from GW signals assuming an $a(t) \propto t$ coasting evolution of the Universe within the redshift range of GW detections. Note that for a fixed k curvature, H_0 is the only parameter of coasting models determining the redshift–distance relation, whereas in the ΛCDM model we need at least one additional parameter (typically the Ω_m present-day matter density parameter) to describe this relationship. As a consequence, GW standard sirens provide tighter constraints on H_0 in coasting models and a more direct way for testing these models compared to the case of the ΛCDM model.

Our paper is organized as follows. In Section 2, we describe the analysis, and the GW and galaxy data we used for our test. In Section 3, we discuss the results of our analyses. Finally, in Section 4, we offer conclusions about our work and the possible ways of continuing it in the future.

Throughout this paper we use $\Omega_m = 0.3065$ and $k = 0$ (and $H_0 = 67.9\ \mathrm{km\ s^{-1}\ Mpc^{-1}}$ where needed) from Ade et al. (2016) for the ΛCDM model, to allow direct comparisons with results published in Abbott et al. (2023a).

2. Data and Analysis

For our tests, we used the publicly available GWTC-3 data (Abbott et al. 2021b) and `gwcosmo` code (Gray et al. 2020; for a more recent and enhanced version of the code, see Gray et al. 2023) to rerun the Abbott et al. (2023a) analysis using the statistical galaxy catalog method adapted to coasting cosmologies.[5] This means that we applied the following relationship between the d_L luminosity distances of the GW sources and the z cosmological redshifts of their host galaxies:

$$d_L(z) = \frac{c}{H_0}(1+z)\begin{cases} \sinh(\ln(1+z)) & \text{for } k=-1 \\ \ln(1+z) & \text{for } k=0 \\ |\sin(\ln(1+z))| & \text{for } k=+1 \end{cases}, \tag{1}$$

where we limited our tests to the three discrete cases of $k = \{-1, 0, +1\}$ for the curvature parameter measured in $H_0^2 c^{-2}$ units (corresponding to $\Omega_0 = \{0, 1, 2\}$ density parameters today, respectively), c being the speed of light in vacuum.

To allow direct comparisons with results published in Abbott et al. (2023a), we analyzed the same 47 GW events from the GWTC-3 catalog that were selected for testing the ΛCDM model there, with matched filter signal-to-noise ratio (S/N) obtained by the LIGO–Virgo detector network S/N > 11 and inverse false-alarm rate IFAR > 4 yr, taking their maximum across the different search pipelines. From this set of GW events, 46 correspond to dark sirens, with GW170817 being the only one originating from a bright siren identified in galaxy NGC4993 at redshift $z = (1.006 \pm 0.055) \times 10^{-2}$ (Abbott et al. 2017c).

Also similarly to Abbott et al. (2023a), we used the `GLADE+`[6] full-sky catalog of over 22 million galaxies and 750 thousand quasars (Dálya et al. 2018, 2022) to select potential host galaxies in our analysis for the dark siren events. Using the measured K_s-band luminosities of galaxies in `GLADE+` (where available), we applied the luminosity weighting described in Abbott et al. (2023a) in our analyses of dark sirens, i.e., we weighted each galaxy with a probability of being the host that is proportional to its K_s-band luminosity.

The code `gwcosmo` uses a Bayesian framework to infer the posterior probability on H_0 from the input GW events. The methodology of the code is explained in detail in Gray et al. (2020). We applied `gwcosmo` in the pixelated sky scheme (Gray et al. 2022) with a pixel size $0.2\ \mathrm{deg}^2$ for analyzing the well-localized GW190814 event (Abbott et al. 2020) and $3.35\ \mathrm{deg}^2$ for all other events. We used the `power law + peak` source mass model (Talbot & Thrane 2018; Abbott et al. 2023b) with the same population parameters used in Abbott et al. (2023a) to describe the primary black hole mass distribution. Also, we used the LIGO and Virgo detector sensitivities during the O1, O2, and O3 observing runs to evaluate GW selection effects. In all analyses, we inferred H_0 using a uniform prior in the interval $H_0 \in [20, 140]\ \mathrm{km\ s^{-1}\ Mpc^{-1}}$. Note that these are the same run settings for `gwcosmo` that were used to produce results in the framework of the ΛCDM model in Abbott et al. (2023a), but limited only to the standard case of the Abbott et al. (2023a) analysis using the most plausible settings. Thus we refer the reader to Abbott et al. (2023a) for a more detailed discussion about the rationale behind the run settings.

H_0 for coasting cosmological models can be determined in a curvature-independent way using the so-called cosmic chronometer or differential age (DA) method originally introduced in Jimenez & Loeb (2002) and Simon et al. (2005). This method takes advantage of the fact that $H(z) = -\dot{z}(1+z)^{-1}$ for all cosmologies (including both the ΛCDM and coasting models) that satisfy $a(z) = (1+z)^{-1}$, and that $\dot{z}$ can in practice be approximated as $\dot{z} \approx \Delta z \Delta t^{-1}$, where Δz and Δt are the

[5] https://github.com/MariaPalfi/gwcosmo_coasting

[6] https://glade.elte.hu/

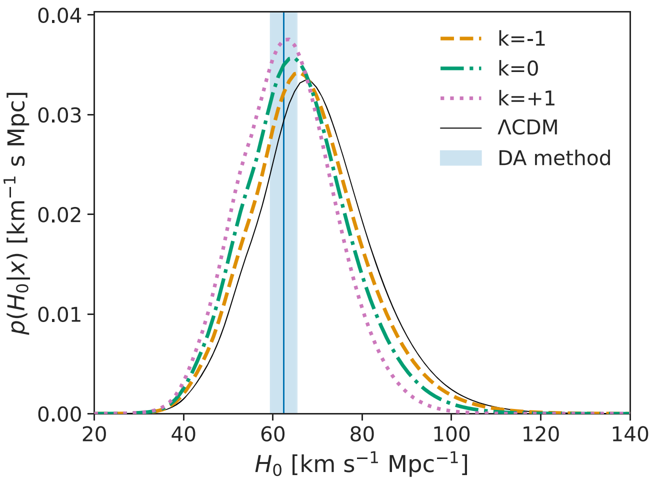

Figure 1. The GW measurements of H_0 from dark siren detections in the first three observing runs of the LIGO–Virgo–KAGRA detector network, assuming coasting cosmologies with $k = \{-1, 0, +1\}$ in $H_0^2 c^{-2}$ units, and the ΛCDM model. The maximum posteriors and 68.3% highest density intervals for H_0 are given in Table 1. We produced all posteriors using uniform priors in the interval $H_0 \in [20, 140]$ km s^{-1} Mpc^{-1}. We also show our estimate of H_0 for coasting cosmologies using the differential age (DA) method, which is $H_0 = 62.41^{+2.95}_{-2.96}$ km s^{-1} Mpc^{-1} regardless of k.

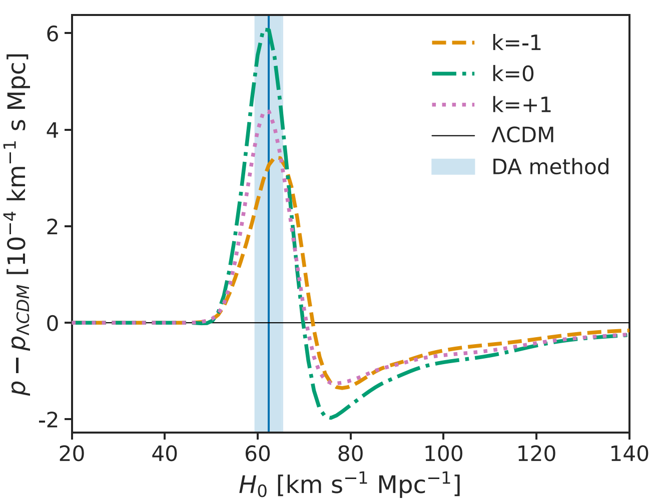

Figure 2. The GW measurements of H_0 from GW170817 (the only bright siren detection in the first three observing runs of the LIGO–Virgo–KAGRA detector network) shown in terms of differences between the p posteriors for H_0 in various cosmologies (including ΛCDM, represented by the solid black line) and the $p_{\Lambda CDM}$ posterior for H_0 in the ΛCDM model. The curves denoted by $k = -1$, $k = 0$ and $k = +1$ correspond to coasting cosmologies with $k = \{-1, 0, +1\}$ in $H_0^2 c^{-2}$ units. We give the maximum posteriors and 68.3% highest density intervals for H_0 in Table 1. We produced all posteriors using uniform priors in the interval $H_0 \in [20, 140]$ km s^{-1} Mpc^{-1}. We also show our estimate of H_0 for coasting cosmologies using the differential age (DA) method, which is $H_0 = 62.41^{+2.95}_{-2.96}$ km s^{-1} Mpc^{-1} regardless of k.

redshift and age differences of, for example, pairs of galaxies at around various z redshifts. Passively evolving galaxies allow measuring their Δt age differences from observed differences in their stellar populations, from which $H(z)$ can be determined with uncertainties typically dominated by uncertainties of the Δt differential age measurement. Melia & Maier (2013) used this DA method to determine H_0 by fitting $H(z) = H_0(1 + z)$ in coasting models to 19 $H(z)$ measurements from Simon et al. (2005), Stern et al. (2010), and Moresco et al. (2012), and obtained $H_0 = 63.2 \pm 1.6$ km s^{-1} Mpc^{-1} regardless of k. We updated their result by fitting the $H(z)$ formula in coasting models to the latest set of 32 $H(z)$ measurements (Simon et al. 2005; Stern et al. 2010; Moresco et al. 2012; Zhang et al. 2014; Moresco 2015; Moresco et al. 2016; Ratsimbazafy et al. 2017; Borghi et al. 2022) summarized in Table 1 of Moresco et al. (2022) using the public `emcee`[7] (Foreman-Mackey et al. 2013) Markov Chain Monte Carlo code with the full statistical and systematic covariance matrix of the data. We obtained $H_0 = 62.41^{+2.95}_{-2.96}$ km s^{-1} Mpc^{-1}, and used this H_0 as a reference for consistency checks of the H_0 posteriors we obtained from GW standard sirens for the coasting models. Note that, in contrast to Abbott et al. (2023a), we cannot use H_0 values obtained by the Planck and SH0ES teams for comparisons (see Aghanim et al. 2020 and Riess et al. 2022, respectively), as both results rely on assumptions valid for the ΛCDM model but not for coasting models.

3. Results

The most distant GW events we analyzed have $d_L \simeq 5$ Gpc (Abbott et al. 2023a), corresponding to $z = 0.78$ in the ΛCDM model, and $z = [0.76; 0.79; 0.83]$ for the $k = \{-1, 0, +1\}$ coasting models with $H_0 = 62.41$ km s^{-1} Mpc^{-1}, respectively. Thus we conclude that our analysis tests all cosmological models with an $a(t) \propto t$ coasting evolution in the redshift range $z \lesssim 0.8$. Since even quasi-linear models propose a coasting evolution in this redshift range, this means that our analyses based on GW standard sirens can test all models in the coasting model family. Note, also, that the tested $z \lesssim 0.8$ redshift range includes $z \simeq 0.64$, when the universe switched from decelerating to accelerating expansion, and $z \simeq 0.30$, when the universe switched from matter-dominated to Λ-dominated expansion in the ΛCDM model, making GW standard sirens excellent tools for making comparisons between expansion histories proposed by the ΛCDM and the coasting models.

In Figure 1, we show the posterior distributions for H_0 in the $k = \{-1, 0, +1\}$ coasting models and in the ΛCDM model we obtained from dark siren detections only. Due to the minor differences between the posterior distributions obtained from the single bright siren detection (GW170817), in Figure 2 we show the differences between the posteriors for H_0 in various cosmologies (including ΛCDM) and the posterior for H_0 in the ΛCDM model. Finally, we show the combined posteriors for H_0 obtained from both dark and bright siren detections in Figure 3. We give the maximum posteriors and 68.3% highest density intervals for H_0 in Table 1, along with the logarithm of the Bayes factors between the tested cosmological models and the ΛCDM model, calculated for all detections. Note that these log Bayes factors are in the order of 10^{-7}–10^{-9} for the three coasting models, which in practice means that all four tested cosmological models fit equally well to the applied set of GW standard siren detections.

The reason for the minor differences in H_0 posteriors for GW170817 is that, originating from a bright siren, both $d_L = 40^{+7}_{-15}$ Mpc (Abbott et al. 2023a) and $z = (1.006 \pm 0.055) \times 10^{-2}$ (Abbott et al. 2017c) for the source are known. We can express H_0 in the coasting models ($H_{0,c}$) and in the ΛCDM model ($H_{0,\Lambda}$) in terms of d_L and z as

$$H_{0,c} \simeq \frac{c}{d_L} z(1 + z)\left[1 - \frac{1}{2}z + \mathcal{O}(z^2)\right] \tag{2}$$

[7] https://gitlab.com/mmoresco/CCcovariance

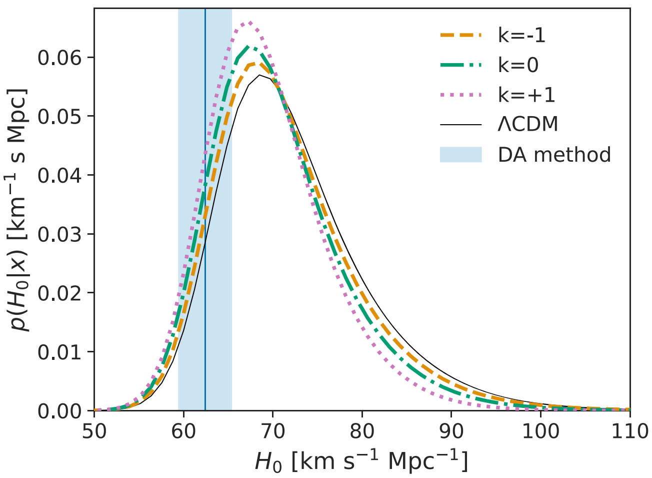

Figure 3. Combined posteriors for H_0 from the dark siren detections and the single bright siren detection (GW170817) in the first three observing runs of the LIGO–Virgo–KAGRA detector network. The curves denoted by $k=-1$, $k=0$, $k=+1$, and ΛCDM correspond to coasting cosmologies with $k=\{-1, 0, +1\}$ in $H_0^2 c^{-2}$ units, and the ΛCDM model, respectively. The maximum posteriors and 68.3% highest density intervals for H_0 are given in Table 1. We produced all posteriors using uniform priors in the interval $H_0 \in [20, 140]$ km s^{-1} Mpc^{-1}. We also show our estimate of H_0 for coasting cosmologies using the differential age (DA) method, which is $H_0 = 62.41^{+2.95}_{-2.96}$ km s^{-1} Mpc^{-1} regardless of k.

Table 1
The GW Measurements of H_0

Model	Dark Sirens	Bright Siren	All Sirens	$\log_{10}\mathcal{B}$ (10^{-8})
$k=-1$	$65.9^{+12.9}_{-11.7}$	$69.3^{+21.2}_{-8.1}$	$68.1^{+8.5}_{-5.6}$	−0.7
$k=0$	$64.5^{+11.6}_{-11.7}$	$69.3^{+21.3}_{-8.0}$	$67.5^{+8.3}_{-5.2}$	11.0
$k=+1$	$63.1^{+10.2}_{-11.5}$	$69.3^{+21.2}_{-8.1}$	$67.1^{+6.6}_{-5.8}$	12.4
ΛCDM	$67.7^{+13.0}_{-12.1}$	$69.4^{+21.2}_{-8.2}$	$68.7^{+8.4}_{-6.3}$	0

Note. The GW measurements of H_0 (maximum posteriors and 68.3% highest density intervals in km s^{-1} Mpc^{-1} units) for coasting cosmologies with $k=\{-1, 0, +1\}$ in $H_0^2 c^{-2}$ units, and for the ΛCDM model.
The second and third columns indicate the H_0 measurements from dark siren detections and from the single bright siren detection (GW170817) in the first three observing runs of the LIGO–Virgo–KAGRA detector network. The fourth column shows the H_0 measurement from all these detections combined. We produced all posteriors using uniform priors in the interval $H_0 \in [20, 140]$ km s^{-1} Mpc^{-1}. In the last column, we show the logarithm of the Bayes factors (in 10^{-8} units) between the tested cosmological models and the ΛCDM model, calculated for all GW siren detections.

$$H_{0,\Lambda} = \frac{c}{d_L}(1+z)\int_0^z \frac{dz'}{\sqrt{\Omega_m(1+z')^3 + 1 - \Omega_m}} \simeq \frac{c}{d_L} z(1+z)\left[1 - \frac{3\Omega_m}{4}z + \mathcal{O}(z^2)\right], \quad (3)$$

and thus

$$H_{0,c} \simeq \left[\frac{1-\frac{1}{2}z}{1-\frac{3\Omega_m}{4}z} + \mathcal{O}(z^2)\right] H_{0,\Lambda}, \quad (4)$$

which for $z \simeq 0.01$ and $H_{0,\Lambda} \simeq 69.4$ km s^{-1} Mpc^{-1} (see Table 1) is $H_{0,c} \simeq 69.2$ km s^{-1}Mpc^{-1}, comparable to the maximum posteriors for H_0 in the coasting models in Table 1.

Similarly to the results presented in Abbott et al. (2023a), the H_0 values we obtained for dark sirens are dominated by the black hole population assumptions we used (see Section 2). As shown in Abbott et al. (2023a), the main source of systematic uncertainty in this case is the choice of the peak location in the `power law + peak` mass model for primary black holes. For all values of k, our H_0 maximum posteriors would decrease with the peak shifting toward lower mass values, and vice versa. This systematic uncertainty can be reduced in the future by using a galaxy catalog in the analysis with a higher level of completeness, by constraining the black hole population model better with the increasing number of GW detections or by jointly estimating parameters of the black hole population model alongside cosmological parameters (Gray et al. 2023; Mastrogiovanni et al. 2023).

4. Conclusions

In this paper, we have presented the first tests of coasting cosmological models with GW standard sirens. We applied the statistical galaxy catalog method with a version of the `gwcosmo` code we adapted to coasting cosmologies, and inferred constraints on H_0, the only parameter of coasting models with fixed values of $k=\{-1, 0, +1\}$, in $H_0^2 c^{-2}$ units. We have presented the H_0 posteriors we obtained using 46 dark siren detections in the first three observing runs of the LIGO–Virgo–KAGRA detector network (see Figure 1), using the single bright siren detection (GW170817; see Figure 2), and for all GW standard siren detections combined (see Figure 3). We have given the maximum posteriors and 68.3% highest density intervals for H_0 in the selected cosmologies in Table 1, along with the log Bayes factors between the tested models and the ΛCDM model, calculated for all GW siren detections. To check the consistency of our results with an independent measurement of H_0, we used $H_0 = 62.41^{+2.95}_{-2.96}$ km s^{-1} Mpc^{-1} as a reference, which we determined for coasting cosmologies independently from k using the DA method. Our results test and constrain all cosmological models with $a(t) \propto t$ linear expansion in the luminosity distance and redshift range of the 47 LIGO–Virgo detections, i.e., $d_L \lesssim 5$ Gpc and $z \lesssim 0.8$, which practically include all (both strictly linear and quasi-linear) models in the coasting model family.

The log Bayes factors in Table 1 indicate that the coasting models and the ΛCDM model fit equally well to the applied set of GW standard siren detections. With the constraints on H_0 we derived, we have found that all $k=\{-1, 0, +1\}$ coasting models are consistent within 1σ with the DA method value of H_0, and that there is an overall trend of the H_0 maximum posterior decreasing with increasing k (thus, the maximum posterior for $k=+1$ is the closest to the H_0 measured with the DA method). Our measurements of H_0, however, with the large error bars, cannot set tight enough constraints on k to exclude any of the three spatial geometries for coasting models from future considerations.

The growing number of GW standard siren detections with the current LIGO–Virgo–KAGRA network (Abbott et al. 2018), soon to be expanded with LIGO-India (Saleem et al. 2022) as well as with future ground-based detectors such as the Einstein Telescope (Punturo et al. 2010) and Cosmic Explorer (Reitze et al. 2019), will allow putting tighter constraints on H_0, with the potential of ruling out certain models in the coasting model family based on their inconsistency with the $d_L(z)$ relation mapped out by GW standard sirens, or with independent determinations of H_0 and k. Additionally, alternative methods developed for measuring H_0 in the ΛCDM model with GW standard sirens (see, e.g., Mastrogiovanni et al. 2021, 2023; also, for a list of existing methods, see the conclusion section of Abbott et al. 2023a and references therein) can be adapted in the future to testing coasting cosmologies and complementing results obtained with the gwcosmo implementation of the statistical galaxy catalog method.

Acknowledgments

The authors thank Juan Casado, Moncy V. John, Fulvio Melia, and Adam Riess for useful comments that improved the manuscript. This paper was reviewed by the LIGO Scientific Collaboration under LIGO Document P2300312. The authors are grateful for the support of the Cosmology and the Tests of ΛCDM subgroups of the LIGO–Virgo–KAGRA Collaboration. This material is based upon work supported by the National Science Foundation's (NSF) LIGO Laboratory, which is a major facility fully funded by the NSF. The authors are grateful for computational resources provided by the LIGO Laboratory and supported by NSF grant Nos. PHY-0757058 and PHY-0823459. This project has received funding from the HUN-REN Hungarian Research Network. This work makes use of gwcosmo, which is available at https://git.ligo.org/lscsoft/gwcosmo.

ORCID iDs

Peter Raffai https://orcid.org/0000-0001-7576-0141
Mária Pálfi https://orcid.org/0000-0001-5942-0470
Gergely Dálya https://orcid.org/0000-0003-3258-5763
Rachel Gray https://orcid.org/0000-0002-5556-9873

References

Aasi, J., Abbott, B. P., Abbott, R., et al. 2015, CQGra, 32, 074001
Abbott, B. P., Abbott, R., Abbott, T. D., et al. 2016, PhRvL, 116, 061102
Abbott, B. P., Abbott, R., Abbott, T. D., et al. 2017a, PhRvL, 119, 161101
Abbott, B. P., Abbott, R., Abbott, T. D., et al. 2017b, ApJL, 848, L12
Abbott, B. P., Abbott, R., Abbott, T. D., et al. 2017c, Natur, 551, 85
Abbott, B. P., Abbott, R., Abbott, T. D., et al. 2018, LRR, 21, 3
Abbott, B. P., Abbott, R., Abbott, T. D., et al. 2021a, ApJ, 909, 218
Abbott, R., Abbott, T. D., Abraham, S., et al. 2020, ApJL, 896, L44
Abbott, R., Abbott, T. D., Acernese, F., et al. 2021b, PhRvX, 13, 041039
Abbott, R., Abe, H., Acernese, F., et al. 2023a, ApJ, 949, 76
Abbott, R., Abbott, T. D., Acernese, F., et al. 2023b, PhRvX, 13, 011048
Acernese, F., Agathos, M., Agatsuma, K., et al. 2015, CQGra, 32, 024001
Ade, P. A. R., Aghanim, N., Arnaud, M., et al. 2016, A&A, 594, A13
Aghanim, N., Akrami, Y., Ashdown, M., et al. 2020, A&A, 641, A6
Akutsu, T., Ando, M., Arai, K., et al. 2021, PTEP, 2021, 05A101
Baumann, D. 2009, arXiv:0907.5424
Benoit-Lévy, A., & Chardin, G. 2012, A&A, 537, A78
Borghi, N., Moresco, M., & Cimatti, A. 2022, ApJL, 928, L4
Casado, J. 2020, Ap&SS, 365, 16
Dalal, N., Holz, D. E., Hughes, S. A., & Jain, B. 2006, PhRvD, 74, 063006
Dálya, G., Díaz, R., Bouchet, F. R., et al. 2022, MNRAS, 514, 1403
Dálya, G., Galgóczi, G., Dobos, L., et al. 2018, MNRAS, 479, 2374
Di Valentino, E., Anchordoqui, L. A., Akarsu, O., et al. 2021, APh, 131, 102604
Dodelson, S. 2003, Modern Cosmology (Amsterdam: Academic Press)
Foreman-Mackey, D., Hogg, D. W., Lang, D., & Goodman, J. 2013, PASP, 125, 306
Fujii, H. 2020, RNAAS, 4, 72
Gray, R., Beirnaert, F., Karathanasis, C., et al. 2023, JCAP, 2023, 023
Gray, R., Hernandez, I. M., Qi, H., et al. 2020, PhRvD, 101, 122001
Gray, R., Messenger, C., & Veitch, J. 2022, MNRAS, 512, 1127
Guth, A. H. 1981, PhRvD, 23, 347
Holz, D. E., & Hughes, S. A. 2005, ApJ, 629, 15
Jimenez, R., & Loeb, A. 2002, ApJ, 573, 37
John, M. V., & Joseph, K. B. 1996, PhLB, 387, 466
John, M. V., & Joseph, K. B. 2000, PhRvD, 61, 087304
John, M. V., & Joseph, K. B. 2023, arXiv:2306.04577
Kaplinghat, M., Steigman, G., Tkachev, I., & Walker, T. P. 1999, PhRvD, 59, 043514
Kaplinghat, M., Steigman, G., & Walker, T. P. 2000, PhRvD, 61, 103507
Lewis, G. F., Barnes, L. A., & Kaushik, R. 2016, MNRAS, 460, 291
MacLeod, C. L., & Hogan, C. J. 2008, PhRvD, 77, 043512
Mastrogiovanni, S., Laghi, D., Gray, R., et al. 2023, PhRvD, 108, 042002
Mastrogiovanni, S., Leyde, K., Karathanasis, C., et al. 2021, PhRvD, 104, 062009
Melia, F. 2007, MNRAS, 382, 1917
Melia, F. 2018, MNRAS, 481, 4855
Melia, F. 2020a, The Cosmic Spacetime (Boca Raton, FL: CRC Press)
Melia, F. 2020b, EPJP, 135, 511
Melia, F. 2022, ApJ, 941, 178
Melia, F., & Maier, R. S. 2013, MNRAS, 432, 2669
Melia, F., & Shevchuk, A. S. H. 2012, MNRAS, 419, 2579
Milne, E. A. 1935, Relativity, Gravitation and World-structure (Oxford: The Clarendon Press)
Moresco, M. 2015, MNRAS, 450, L16
Moresco, M., Amati, L., Amendola, L., et al. 2022, LRR, 25, 6
Moresco, M., Cimatti, A., Jimenez, R., et al. 2012, JCAP, 2012, 006
Moresco, M., Pozzetti, L., Cimatti, A., et al. 2016, JCAP, 2016, 014
Nissanke, S., Holz, D. E., Dalal, N., et al. 2013, arXiv:1307.2638
Peebles, P. J., & Ratra, B. 2003, RvMP, 75, 559
Perivolaropoulos, L., & Skara, F. 2022, NewAR, 95, 101659
Punturo, M., Abernathy, M., Acernese, F., et al. 2010, CQGra, 27, 194002
Ratsimbazafy, A. L., Loubser, S. I., Crawford, S. M., et al. 2017, MNRAS, 467, 3239
Reitze, D., Adhikari, R. X., Ballmer, S., et al. 2019, BAAS, 51, 35
Riess, A. G. 2020, NatRP, 2, 10
Riess, A. G., Yuan, W., Macri, L. M., et al. 2022, ApJL, 934, L7
Saleem, M., Rana, J., Gayathri, V., et al. 2022, CQGra, 39, 025004
Schutz, B. F. 1986, Natur, 323, 310
Sethi, M., Batra, A., & Lohiya, D. 1999, PhRvD, 60, 108301
Simon, J., Verde, L., & Jimenez, R. 2005, PhRvD, 71, 123001
Soares-Santos, M., Palmese, A., Hartley, W., et al. 2019, ApJL, 876, L7
Stern, D., Jimenez, R., Verde, L., Stanford, S. A., & Kamionkowski, M. 2010, ApJS, 188, 280
Talbot, C., & Thrane, E. 2018, ApJ, 856, 173
Zhang, C., Zhang, H., Yuan, S., et al. 2014, RAA, 14, 1221